

New, Lead Free, Perovskites With a Diffuse Phase Transition: NaNbO_3 Solid Solutions

I. P. Raevski and S. A. Prosandeev

Department of Physics, Rostov State University, 5 Zorge Street, 344090, Rostov on Don, Russia

Abstract. Some of $(1-x)\text{NaNbO}_3 - (x)\text{ABO}_3$ perovskite solid solutions exhibit a dramatic diffusion of the dielectric permittivity ε' maximum and relaxor-type behavior when the second component concentration exceeds a threshold value x_0 . The concentration phase transition to the relaxor-like phase is abrupt (of the first order kind) that is seen from the step in the dependence of the $\varepsilon'(T)$ maximum temperature, T_m , on x . The precursor of this transition is a giant (up to 100 K) temperature hysteresis of $\varepsilon'(T)$. Some relaxor-like properties appear even at $x < x_0$ in the course of cooling while disappear in the course of heating. The experimental data obtained are qualitatively described within a Landau-type phenomenological approach, assuming the relaxor-type behavior to be local stress-induced.

I INTRODUCTION

The relaxor behavior in perovskites was studied predominantly in Pb-containing ternary compounds (PMN, PST, PSN) and solid solutions (PLZT, PMN-PT) [1-3]. Last years some lead-free BaTiO_3 -derived solid solution compositions attracted much attention as environmentally benign relaxor materials [4]. However up to now the obtained values of the dielectric permittivity ε' maximum temperature, T_m , in the BaTiO_3 -based relaxors were too low for potential applications [4]. The aim of the present paper is studying the dielectric properties of some NaNbO_3 -based solid solutions forming a new family of lead-free materials with diffuse phase transition (DPT).

On heating NaNbO_3 exhibits a series of six phase transitions from the low temperature ferroelectric (FE) phase N ($R3c$) to the high temperature paraelectric (PE) cubic phase U ($Pm3m$) through different antiferroelectric (AFE) and PE phases [5]. An $\varepsilon(T)$ maximum originating from the first order transition between two AFE phases: $P(Pbma)$ and $R(Pmnm)$ is observed at 350-370⁰C.

Similar to solid solutions of other perovskite antiferroelectrics, the NaNbO_3 - ABO_3 binary solid solution systems can be divided into two groups [6]. In the solid solutions of group I (e.g. $(\text{Na,Li})\text{NbO}_3$ and $(\text{Na,K})\text{NbO}_3$ systems) the high

temperature FE phase appears at small (a few mol.%) content x of the second component ABO_3 , the $T_m(x)$ dependence is rather smooth and the $\varepsilon'(T)$ maxima are sharp. In the solid solutions of group II the AFE phase remains stable up to a comparatively high x values. In contrast to the solid solutions of other perovskite antiferroelectrics, the $T_m(x)$ dependence of the NaNbO_3 -based group II solid solutions remains smooth only up to a threshold $x = x_0$ value. At $x > x_0$ the phase, usually referred to as FE (though sometimes it is supposed to be ferrielectric), becomes stable, which is accompanied by an abrupt drop in the T_m values and dramatic diffusion of the $\varepsilon'(T)$ maximum. While the T_m values of the compositions with $x < x_0$ do not depend on frequency, the compositions with $x > x_0$ were reported to exhibit a frequency dispersion of ε' and an increase of T_m with frequency [6]. Thus, it seems that NaNbO_3 -based solid solutions belonging to group II exhibit a relaxor-like behavior at $x > x_0$. Besides, the lack of systematic data on the properties of such materials prevents one from definite conclusions. Below we will consider some group II NaNbO_3 -based solid solutions dielectric properties dependence on the concentration of the second and third components as well as on temperature and frequency.

II EXPERIMENTAL RESULTS

NaNbO_3 - $\text{Gd}_{1/3}\text{NbO}_3$ solid solution crystals were grown by the flux method. The details of crystal preparation and characterization have been described elsewhere [7]. The ceramic samples of NaNbO_3 -based solid solutions were prepared by routine solid-state reaction route. The density of the obtained ceramics was about 90-95 % of theoretical one. For dielectric measurements Aquadag electrodes were deposited on the opposite faces of the as-grown crystals, while Ag paste was fired to the grinded disk surfaces of ceramic samples. The dielectric studies were carried out in the 1 kHz -1 MHz range in the course of both heating and cooling at a rate of 2 -3 °C/min with the aid of the *R5083* and *E7 - 12* capacitance bridges.

Fig. 1 shows the typical evolution of the $\varepsilon'(T)$ dependencies with the composition for the solid solution of group II. The similarity of the data obtained for ceramic samples and crystals shows that the peculiar properties of the group II solid solutions are not due to the immiscibility effect typical of many solid solution ceramics. A strong frequency dispersion of both real (ε') and imaginary (ε'') parts of complex dielectric permittivity observed at temperatures exceeding T_m or T_m'' (Fig. 2) is likely to be caused by a decrease of the conductance influence with increasing frequency. Though the $\varepsilon'(T)$ maxima of the group II NaNbO_3 -based solid solution compositions with $x > x_0$ are smeared and a frequency dispersion of ε' is observed, the shift of T_m with frequency is usually much smaller than in the case of $\text{PbMg}_{1/3}\text{Nb}_{2/3}\text{O}_3$ -type relaxors (Fig.2). Similar to other FE and AFE with DPT [1-3], the permittivity of NaNbO_3 -based solid solution compositions with $x > x_0$ does not follow the Curie-Weiss law in a broad temperature range above T_m (Fig. 2) while at higher temperatures the Curie-Weiss behavior is observed. It

is well documented that in FE with DPT the extrapolated Curie-Weiss temperature of the FE phase transition, T_{CW} , is necessarily higher than T_m due to a large contribution to the high-temperature permittivity from the regions that have a higher transition temperature [1-3]. In contrast to this, in all the group II NaNbO₃-based solid solutions studied, the T_{CW} values are much lower than T_m (Fig.2). Figure 3 shows the concentration dependencies of T_m measured on heating for some solid solutions belonging to group II. It is interesting to note that for many solid solution systems of group II the linear extrapolations of the $T_m - x$ diagram portions from the $x > x_0$ region intersect at the same point ($x = 0, T \sim 150^\circ\text{C}$) corresponding to the minor $\varepsilon'(T)$ anomaly often observed in NaNbO₃ [8].

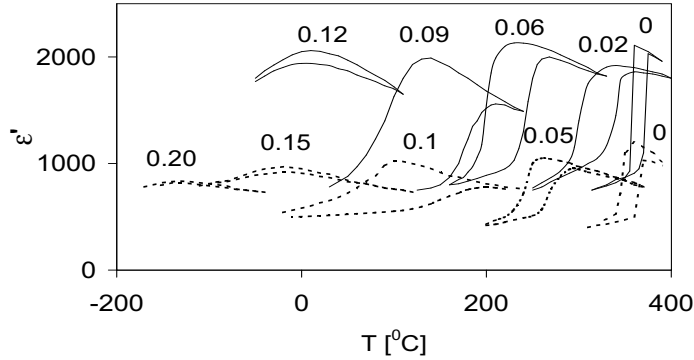


FIGURE 1. Evolution of the $\varepsilon'(T)$ dependencies measured on heating and subsequent cooling with composition for $(1-x) \text{NaNbO}_3\text{-}x\text{Gd}_{1/3}\text{NbO}_3$ single crystals (solid lines) and ceramics (dashed lines). Figures correspond to x values.

A specific feature of the group II solid solutions is an anomalously large value of the thermal hysteresis ΔT_h of the $\varepsilon'(T)$ dependence typical of the compositions with $x < x_0$. The ΔT_h values increase with x and in some systems exceed 100 K for compositions adjacent to x_0 (Figs. 1, 4). The concentration dependence of ΔT_h is substantially nonlinear (Fig. 4). When a small amount of FE third component is added to the given solid solution, ΔT_h values usually increase [10-12]. At higher FE component content the ΔT_h values decrease dramatically [11]. If the temperature is stabilized in the course of cooling within the thermal hysteresis range the temporal changes in ε' do not exceed a few % during several hours [12]. Application of DC bias on compositions exhibiting giant ΔT_h values does not change the $\varepsilon'(T)$ curve measured in the heating mode while in the course of subsequent cooling some lowering of the $\varepsilon'(T)$ maximum was observed [12,13]. Anomalously large values of ΔT_h were observed both in the ceramics and single crystals and can serve as an experimental evidence of the fact that the given solid solution belongs to group II [7,9,11]. It is worth noting that in perfect NaNbO₃ single crystals the ΔT_h value does not exceed 10 K, but increases substantially with

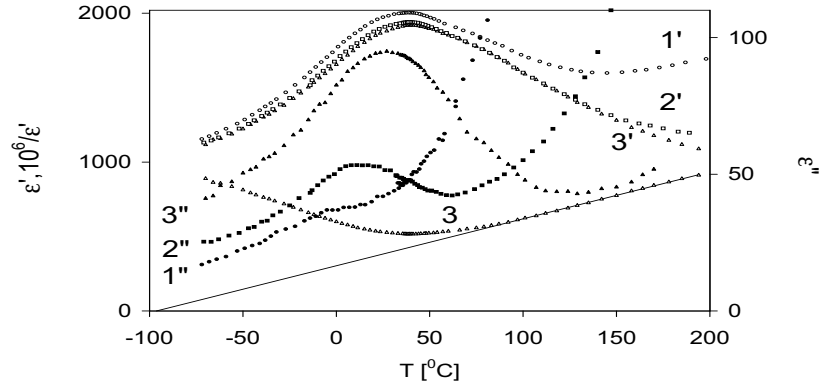


FIGURE 2. Temperature dependencies of ε' (1'-3'), ε'' (1''-3'') and $10^6/\varepsilon'$ (3) measured at 1 kHz (1',1''), 10 kHz (2',2'') and 100 kHz (3,3',3'') for $0.88\text{NaNbO}_3\text{-}0.12\text{Gd}_{1/3}\text{NbO}_3$ single crystal

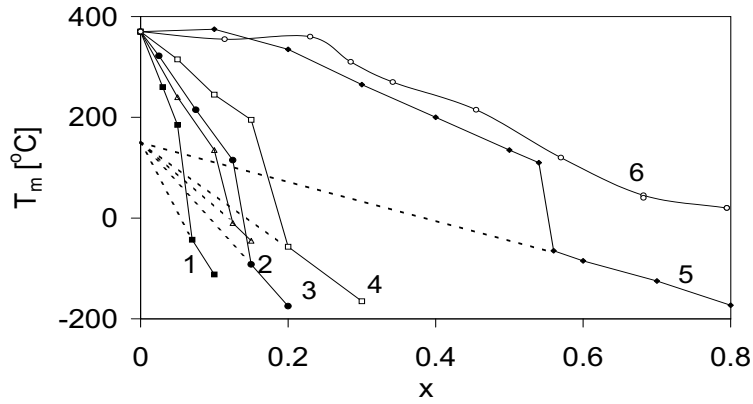


FIGURE 3. Concentration dependencies of the $\varepsilon'(T)$ maximum temperature T_m measured on heating for some NaNbO_3 -based solid solutions belonging to the group II (1-5) as well as for $0.88\text{NaNb}_{1-x}\text{Ta}_x\text{O}_3\text{-}0.12\text{LiNbO}_3$ [16] system (6). The second components of the solid solutions are: 1. BiFeO_3 ; 2. $\text{SrCu}_{1/3}\text{Nb}_{2/3}\text{O}_3$; 3. CaTiO_3 [17]; 4. SrTiO_3 [23]; 5. NaTaO_3 [24];

the increase of the oxygen vacancy concentration [14]. In nominally stoichiometric NaNbO_3 ceramics the ΔT_h values of 30 - 40 K are usually observed (Fig. 1). These larger values of ΔT_h in ceramic samples are likely to be attributed to a high point-defect concentration, e.g. due to evaporation of Na_2O during sintering. Indeed, in Na_2O -deficient $\text{Na}_{1-x}\text{NbO}_{3-x/2}$ ceramics [15] the ΔT_h values are substantially larger than in the nominally stoichiometric ones. Both the oxygen- and Na_2O -deficiency leads to an increase of the T_m values in NaNbO_3 [14,15] and an almost linear correlation of ΔT_h and T_m is observed.

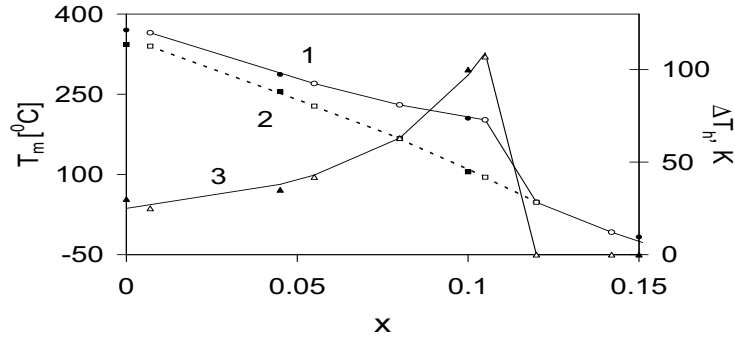


FIGURE 4. Concentration dependence of the $\varepsilon'(T)$ maximum temperature T_m measured on heating (1) and on cooling (2) as well as the $\varepsilon'(T)$ temperature hysteresis ΔT_h values (3) for $(1-x)\text{NaNbO}_3-x\text{Gd}_{1/3}\text{NbO}_3$ crystals (open symbols) and ceramics (filled symbols)

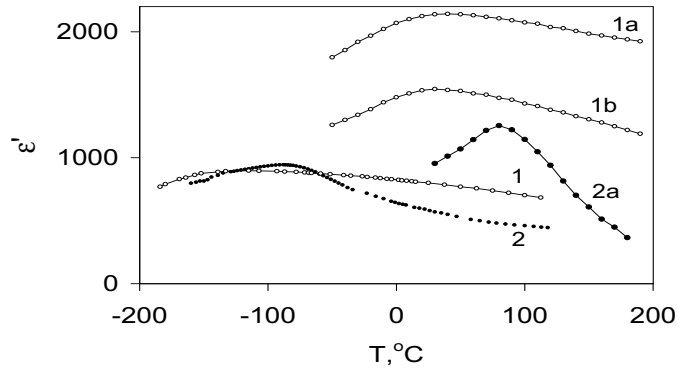


FIGURE 5. Changes in the $\varepsilon'(T)$ dependencies of $0.8\text{NaNbO}_3-0.2\text{Na}_{0.5}\text{Bi}_{0.5}\text{TiO}_3$ (1) and $\text{NaNb}_{0.45}\text{Ta}_{0.55}\text{O}_3$ (2) solid solution ceramics caused by addition of 10 mol% of LiNbO_3 (curves 1a and 2a) or KNbO_3 (1b). Curve 2a is drawn using the data of Ref. [16].

It should be mentioned that a noticeable step in the $T_m(x)$ dependence of the

NaNbO₃-based solid solutions belonging to group II is observed only for the T_m values measured in the heating mode. If T_m is determined from the $\varepsilon'(T)$ dependence measured in the course of cooling, the $T_m(x)$ curve is rather smooth (Fig. 4). The $\varepsilon'(T)$ dependencies measured in the cooling mode are usually more diffused as compared to those measured upon heating (Fig.1). Moreover, just at the step in the $T_m(x)$ dependence the $\varepsilon'(T)$ curve obtained on cooling down has a relaxor-like diffuse maximum that can imply that the relaxor-type state had been already appeared in a metastable thermodynamic state occupied at cooling. The stability of this state arises at temperatures lower than the step in the $T_m(x)$ dependence. In the latter case (i.e. for the compositions with $x > x_0$) the curves obtained in the cooling and heating modes practically coincide.

As one can see from Figs. 1 and 3, the T_m values of the known binary NaNbO₃-based relaxor-type solid solutions, belonging to group II, are usually well below the room temperature, and the maximal ε' values, ε'_m , are much lower than in the Pb-containing relaxors. However, in the ternary NaNbO₃-NaTaO₃-LiNbO₃ solid solution system a dramatic increase in both the T_m and ε'_m values with the LiNbO₃ content is observed [16] for the compositions from the $x > x_0$ range (Figs. 3 and 5). Similar behavior is typical of other NaNbO₃-based solid solutions (Fig. 5).

III DISCUSSION

When discussing the experimental data we will use a phenomenological Landau-type approach. For the sake of simplicity we do not follow the complex symmetry of the NaNbO₃-based solid solutions but rather, in order to make a qualitative description, we consider a simplified case when there are two nonpolar (AFE) (Q_1 , and Q_2) and one polar (FE) (P) order parameters. An important constraint on the Free energy expansion is that an AFE phase transition may exhibit a peak or step in the $\varepsilon'(T)$ only because of coupling between FE and AFE order parameters [18,19]. The impurities we consider are expansive that implies that they produce local random stress (σ_l) leading to a local expansion of the lattice parameter and, hence, to local strain (e). The small observed dispersion of $\varepsilon'(T)$ at $x > x_0$ requires the introduction of an additional parameter (d), which is the local mean square impurity- induced dipole (or multipole) moment. We assume that local expansion around a defect may lead to noncentrosymmetric relaxations of neighboring atoms yielding a net local moment, or a multipolar set of local moments. Averaged over the whole crystal, these relaxations do not generate a net macroscopic moment but local moments cause dispersion of $\varepsilon'(T)$. Extended dipole-dipole interactions are assumed to be sufficiently weak that they can be ignored.

We expand the Free energy as a sum of x -independent (F_1) and x -dependent (F_2) contributions, $F = F_1 + xF_2$ where

$$\begin{aligned}
F_1 = & F_0 + \frac{1}{2}\alpha_{11}(T)P^2 + \frac{1}{4}\beta_1P^4 - EP + \\
& + \frac{1}{2}\alpha_{21}(T)Q_1^2 + \frac{1}{2}\alpha_{22}(T)Q_2^2 - \frac{1}{4}\beta_{21}Q_1^4 + \frac{1}{4}\beta_{22}Q_2^4 + \frac{1}{6}\gamma_{21}Q_1^6 + \\
& + \frac{1}{2}\beta_{121}P^2Q_1^2 + \frac{1}{2}\beta_{122}P^2Q_2^2
\end{aligned} \tag{1}$$

$$F_2 = \frac{1}{2}c_L e^2 - \sigma_l e - \frac{1}{2}a_1 e P^2 + \frac{1}{2}a_{21} e Q_1^2 + \frac{1}{2}a_{22} e Q_2^2 - \lambda d e + \frac{1}{2}\kappa d^2$$

Here $\alpha_i = c_1(T - T_1^{(0)})$, $\alpha_{2i} = c_{2i}(T - T_{2i}^{(0)})$, $T_1^{(0)}$ and $T_{2i}^{(0)}$ are the bare Curie temperatures for the FE and for AFE phase transitions respectively, E is external electric field, e is the symmetrical part of the strain tensor. From the equilibrium condition with respect to e and d one has

$$\begin{aligned}
e &= \frac{1}{c_L} \left(\sigma_l + \lambda d + \frac{1}{2}a_1 P^2 - \frac{1}{2}a_{21} Q_1^2 - \frac{1}{2}a_{22} Q_2^2 \right) \\
d &= \lambda e / \kappa
\end{aligned} \tag{2}$$

It implies that d multiplied by λ plays the role of the local stress and hence it effectively enlarges the local stress produced by impurities, d proves to be proportional to the strain e . From (1) and (2) one can easily find that e (as well as d , see [20]) is enhanced due to mutual coupling between e and d :

$$e = \frac{1}{c_L - \lambda^2/\kappa} \left(\sigma_l + \frac{1}{2}a_1 P^2 - \frac{1}{2}a_{21} Q_1^2 - \frac{1}{2}a_{22} Q_2^2 \right) \tag{3}$$

By using (3) one can rewrite Free energy in the simple form containing expansions only with respect to P and Q :

$$\begin{aligned}
F = & F'_0 + \frac{1}{2}A_1(x, T)P^2 + \frac{1}{4}B_1(x)P^4 - EP + \frac{1}{2}A_{21}(x, T)Q_1^2 + \\
& \frac{1}{2}A_{22}(x, T)Q_2^2 - \frac{1}{4}B_{21}(x)Q_1^4 + \frac{1}{6}\Gamma_2(x)Q_1^6 + \frac{1}{4}B_{22}(x)Q_2^4 + \\
& \frac{1}{2}B_{121}(x, T)P^2Q_1^2 + \frac{1}{2}B_{122}(x, T)P^2Q_2^2 + \dots
\end{aligned} \tag{4}$$

where $F'_0 = F_0 - x\sigma_l^2/2\varsigma$ and coefficients A and B depend on concentration, e.g.

$$\begin{aligned}
B_{21}(x) &= \beta_{21} + xa_{21}^2/2\varsigma \\
B_{121}(x) &= \beta_{121} + xa_1a_{21}/2\varsigma \\
B_{122}(x) &= \beta_{122} + xa_1a_{22}/2\varsigma
\end{aligned} \tag{5}$$

Here $\varsigma = (c_L - \lambda^2/\kappa)^2/c_L$. We have obtained that the coupling of the order parameter Q_i with the strain e produced by the impurities leads to the dependence of the coefficients in the Landau expansion on the concentration x (see also [21]).

Composition dependence in coefficients (5) implies that the Curie temperature also depends on x :

$$\begin{aligned}
T_1 &= T_1^{(0)} + x\sigma_l a_1 / c_1 \varsigma \\
T_{2i} &= T_{2i}^{(0)} - x\sigma_l a_{2i} / c_{2i} \varsigma
\end{aligned} \tag{6}$$

From these expressions it is seen that if $a_1 > 0$ and $a_2 > 0$ then T_1 increases with x and T_2 decreases with x linearly. The latter result corresponds to the

experimental data: all group II NaNbO₃-based solid solutions studied exhibit a decrease in T_m with x . The assumed signs of a_1 and a_2 are natural as the electrostrictive constant a_1 is always positive (if in the F one puts the sign "-" in front of it) and a_2 should also be positive (if one puts the sign "+" in front of it) because compression of the lattice ($e < 0$) typically promotes AFE order while the expansion ($e > 0$) promotes FE order.

From expansion (4) one can easily obtain: the critical temperature of the AFE phase transition, T_{Ai} ; the temperature hysteresis width, ΔT_h ; and the jump of the AFE order parameter, ΔQ_1 :

$$\begin{aligned} T_{A1} &= T_{21} + 3B_{21}^2/16c_{21}\gamma_{21} - B_{121}P^2/c_{21} \\ T_{A2} &= T_{22} - B_{122}P^2/c_{22} \\ \Delta T_h &= B_{21}^2/4c_{21}\gamma_{21} \\ \Delta Q_1 &= \sqrt{B_{21}/2\gamma_{21}} \end{aligned} \quad (7)$$

From (6) it is clear that T_{2i} is a linear function of x , which implies that $T_{Ai}(x)$ is also linear at small x . This corresponds to the experimentally observed linear decrease of $T_m(x)$ with x both above and below x_0 as well as explains why linear extrapolations to the point $x = 0$ for various second components, intersect at one point (Fig. 3). These points correspond to the bare Curie temperatures $T_{2i}^{(0)}$. The slopes of the linear dependencies above and below x_0 are different as are the electrostriction constants ($a_{21} > a_{22}$). Thus: Curie lines $T_{A1}(x)$ and $T_{A2}(x)$ intersect at $x = x_0$; Q_1 is nonzero for $T < T_{A1}$ ($x < x_0$); Q_2 is nonzero for $T < T_{A2}$ ($x_0 < x$). The point $x = x_0$ can be found from the equality: $T_{A1}(x) = T_{A2}(x)$.

At the intersection of curves $T_{A1}(x)$ and $T_{A2}(x)$, the first order phase transition to the AFE phase, with order parameter Q_1 , intersects the second order phase transition to the AFE phase, with order parameter Q_2 , at a *critical endpoint* [22]. The principle experimental evidence supporting this interpretation is that the thermal hysteresis vanishes abruptly at x_0 (Fig.4). Note that we assume $B_{21} > 0$ and $B_{22} > 0$ but the sign "-" stands in (4) in front of B_{21} and "+" precedes B_{22} . The alternative assumption, that there is a tricritical point at $(x_0, T_{Ai}(x))$, would imply a *gradual disappearance* of the thermal hysteresis as x approaches x_0 from below.

Strong x -dependence of the thermal hysteresis at $x < x_0$ is unusual. From (5) it follows that B_{21} increases with x regardless of the sign of the electrostriction constant. At small x , this leads to a linear increase in $\Delta T_h(x)$ while at larger x , $\Delta T_h(x)$ increases quadratically, in excellent agreement with experiment (Fig.4).

From (7) it follows that the jump, ΔQ_1 , in AFE order parameter Q_1 should depend on the concentration x . Because B_2 increases linearly with x , so must ΔQ_1 . Experimentally, it is observed that as x increases, so does the difference between the magnitudes of ϵ'_m measured on cooling and on heating (Fig.1), which implies good agreement between theory and experiment.

Our data are insufficient to identify the crystal structure of the AFE phase associated with $Q_2=finite$ ($x_0 < x$) but some properties are clear: $\varepsilon'(T)$ is relaxor-like with a diffuse maximum and dispersion below T_m . Some properties however, are not typically relaxor-like: the dielectric permittivity magnitudes are much lower than those in typical relaxors such as PMN; the $\varepsilon'(T)$ fits the Curie-Weiss law well above T_m , but the extrapolated Curie-Weiss temperature, T_{CW} , is significantly below T_m rather than above as in typical relaxors; in spite of the dramatic diffusion of $\varepsilon'(T)$, the frequency dependence of ε' and T_m is much weaker than in typical relaxors. The comparatively small magnitude of ε'_m can be connected with the absence of the large contribution of lead to the dielectric permittivity.

IV SUMMARY

From the discussion above it follows that one of the main reasons for the appearance of the relaxor-like properties in the NaNbO₃-based solid solutions belonging to group II can be the appearance of the (random) local strain (with nonvanishing average magnitude) stemmed from the impurities. Due to the electrostriction effect this results in the decrease of the AFE critical temperature, increase of the thermal hysteresis width with x , and, finally, with the appearance of a new diffuse phase transition with weak dispersion of the dielectric permittivity. Large diffusion of the $\varepsilon'(T)$ maxima in some solid solution compositions with $x > x_0$ and the possibility of shifting T_m to the room temperature range in conjunction with relatively weak frequency dependence of both T_m and ε'_m may be of certain interest for applications. The same is true for solid solution compositions with $x < x_0$ exhibiting giant $\varepsilon'(T)$ thermal hysteresis values.

V ACKNOWLEDGMENTS

This work was partially supported by Russian Foundation for Basic Research (Grants # 01-03-33119 and 01-02-16029). S.A.P. appreciates discussions with M. Glinchuk and B. Burton.

REFERENCES

1. Cross, L. E., *Ferroelectrics* **76**, 241-267 (1987).
2. Cross, L. E., *Ferroelectrics* **151**, 305-320 (1994).
3. Chen, I. -W., Li, P., and Wang, Y., *J. Phys. Chem. Solids*, **57**, 1525-1536 (1996).
4. Ravez, J., and Simon, A., *J. Korean Phys. Society*, **32**, S955-S956 (1998).
5. Megaw, H. D., *Ferroelectrics* **7**, 87-89 (1974).
6. Krainik, N. N., *Izv. Akad. Nauk SSSR, Ser. Fiz.* **28**, 643-648 (1964). (in Russian).
7. Raevski, I. P., Smotrakov, V. G., Lisitsina, S. O., Zaitsev, S. M., and Selin, S. V., *Inorganic Materials*, **21**, 734-736 (1985).

8. Raevski, I. P., Resnitchenko, L. A., Smotrakov, et. al., *Tech. Phys. Letters*, **26**, 744-746 (2000).
9. Lisitsina, S.O., Raevski, I.P., and Gegusina, G.A., *Sov. Phys.-Tech. Physics*, **319**, 673-675 (1986).
10. Metayer, S., Von der Mühl, R., Ravez, J. , and Hagenmuller, P., *C. r. Acad. Science*, **C284**, 723-726 (1977).
11. Raevski, I. P., Emelyanov, S. M., Servuli, V. A., Lisitsina, S.O., and Totmyanin, A. A., *Sov. Phys. -Tech. Physics*, **29**, 587-589 (1984).
12. Korotkov, L. N., Gridnev, S. A., Kleshchenko, V. A., Belousov, M. A., and Raevski, I. P., submitted to *Ferroelectrics*.
13. Drobisheva, L. A., Viskov, A. S., and Venevtsev, Yu. N., *Elektronnaya Tekhnika. Ser. Materiali*, **4(7)**, 62-69 (1969). (In Russian).
14. Molak, A., *Solid State Communications*, **62**, 413-417 (1987).
15. Lisitsina, S.O., Raevski, I. P., Maksimov, S. M., Resnitchenko, L. A., and Shilkina, L. A., *Inorganic Materials* **21**, 865-868 (1985).
16. Palatnikov, M., Voloshina, O., Serebryakov, J., Kalinnikov, V., Bormanis, K., and Stefanovich, S., *Ferroelectrics*, **131**, 227-232 (1992).
17. Glaister, R. M., *J. Amer. Ceram. Society*, **43**, 348-353 (1960).
18. V. G. Vaks, *Vvedenie v mikroskopicheskuyu teoriyu segnetoelektrikov*, Moscow, Nauka, 1973 (in Russian).
19. Stephanovich, V. A., Glinchuk, M. D., Jastrabik, L., *Ferroelectrics*, **240**, 343-353 (2000).
20. Pirc, R., and Blinc, R., *Phys. Review*, **B83**, 13470-13478 (1999).
21. Molak, A., *J. Phys.: Condens. Matter*, **9**, 11263-11282 (1997).
22. Allen, S. M., and Cahn, J. W., *Bulletin of Alloy Phase Diagrams*, **3**, 287 (1982).
23. Krainik, N. N., *Izv. AN SSSR, Ser. Fiz.* **22**, 1492-1496 (1958). (in Russian).
24. Iwasaki, H., *Rev. Electr. Commun. Lab.* **12**, 469-487 (1964).